

# Effects of Receiver Input Impedance on Nonlinear Distortion in Full-duplex Radios

Xichen Li

Department of Electrical Engineering  
University of Washington  
Seattle, WA USA  
xcli@uw.edu

Fucheng Yin

Department of Electrical Engineering  
University of Washington  
Seattle, WA USA  
yin4444@uw.edu

Jacques C. Rudell

Department of Electrical Engineering  
University of Washington  
Seattle, WA USA  
jcrudell@uw.edu

**Abstract**—This paper explores and models the generation of nonlinearities arising from common- and differential-mode transmitter (TX) self-interference (SI) at the input of full-duplex (FD) radio receivers (RX). The analysis reveals the impact of residual TX-SI which drives the RX input impedance ( $Z_{rx}$ ), generating distortion products that degrade the RX linearity. Circuit simulation results confirm a nonlinear  $Z_{rx}$  introduces non-negligible distortion at the RX input from the residual TX-SI. To suppress the total distortion below the RX noise floor, SI mitigation circuits at RF front-end must provide at least 60dB SI suppression and 50dB common-mode isolation to achieve sufficient RX linearity performance. This paper draws conclusions with respect to strategies that allow a reduction in the nonlinearities generated at the RX input due to residual TX-SI as would be found in FD transceivers.

**Index Terms**—Radio frequency, interference suppression, intermodulation distortion, receivers (RX), CMOS integrated circuits.

## I. INTRODUCTION

Evolving 5th generation (5G) standards continue to drive the demand for higher data rate wireless transceivers to meet the increasing BW needs of future applications such as cloud computing and Internet-of-Things (IoT) [1]. Full-duplex (FD) communication systems, capable of simultaneously transmitting and receiving on the same channel, have evolved to address some of these future high-data rate demands. However, mitigating transmitter (TX) self-interference (SI) present at the receiver (RX) front-end remains a major challenge [2]–[4]. The TX leakage which directly couples into the RX input has the shortest delay and highest magnitude, thus the demands on RX linearity are placed at the RX input interface where numerous methods have been explored to improve the TX-to-RX isolation [4]–[9]. An ideal SI mitigation circuit should provide high SI suppression with high linearity. Any nonlinear distortion injected by the SI-mitigation circuit blocks act to degrade the RX sensitivity. Recently, research groups have reported high linearity cancelers using all-passive integrated electrical balance duplexers (EBD) [5], [6], however most of these efforts measure the  $IP_3$  of a standalone duplexer, deviating from the practical case when the duplexer is interfaced to the RX chain. While traditional measures of distortion at RX input take into account the nonlinearities generated in the RX chain, referred back to the input, and the distortion produced

by SI mitigation circuits, this paper examines the effects of a nonlinear RX input impedance ( $Z_{rx}$ ) present at the differential receiver input, as would be the case with a strong residual TX-SI at the RX input. Contributions to nonlinear  $Z_{rx}$  mainly include the input device transconductance ( $g_m$ ) looking into the LNA and the junction capacitance at the RX input.

This work investigates the effect of both differential and common-mode residual SI on distortion generated at the RX input. Of particular interest is the often overlooked effect of common-mode TX-SI generating differential intermodulation products. To the best of our knowledge, this is the first attempt to model and verify through circuit simulation the distortion generated by nonlinear  $Z_{rx}$  at the RX input. An understanding of the intermodulation components generated right at the RX input is critical to understand the RX performance in the presence of TX strong interference.

Section II of this paper gives a detailed description for the unique situation of nonlinear distortion generated at the RX input, in the presence of a strong TX-SI. Section III examines the impact of large common-mode TX leakage on the differential nonlinear distortion using an analytical model, which is verified through circuit simulation in Section IV. Concluding comments are provided in Section V.

## II. TX-SI INDUCED INTERMODULATION AT THE RX INPUT

### A. Linearity Requirements of Full-duplex Radios

WiFi is a common wireless standards and makes an excellent candidate for FD applications given the continued demand for higher data rates. A commonly used TX output power for WiFi is +15dBm to +20dBm [10] which makes the linearity of FD applications challenging. An additional linearity challenge relates to the fact that many standards now use multi-carrier modulation. The use of many sub-carriers within the channel bandwidth further increases the linearity demand of the transmitter, receiver and any SI mitigation circuitry. Fig.1 shows the SI mitigation at the RF front-end in FD transceivers, where the PA delivers a high power signal that is fed into the SI mitigation circuits and is coupled to the RX input. SI mitigation circuits and RX front-end with limited linearity can generate numerous intermodulation cross-products at RX input. For example, if a PA transmits a two-tone signal at the canceler input (15dBm each tone),

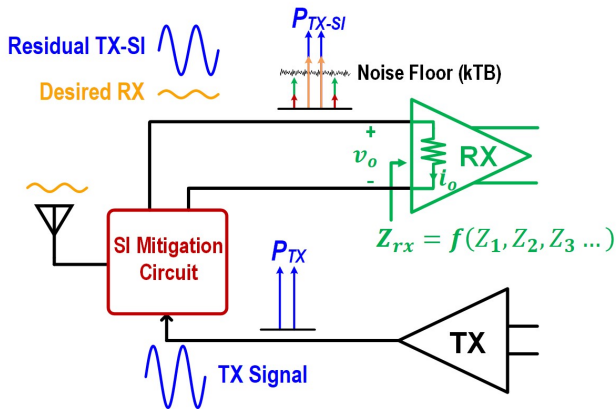


Fig. 1. Intermodulation distortion generated at the RX input in the presence of TX-SI in FD transceivers. Intermodulation components in red and in green are introduced from SI mitigation circuits and nonlinear  $Z_{rx}$ , respectively.

assuming both -90dBm RX noise floor and at least 10dB of margin, the third order intermodulation ( $IM_3$ ) products must be below -100dBm. For 30dB SI suppression between the TX and the RX, the required input  $IP_3$  referred to the TX output is +57.5dBm which is most challenging to realize in practice.

### B. Radio Air Interface Sources of Distortion

Distortion at the RX input, generated by SI mitigation circuits, has been discussed in [5], [11]. In this section, the distortion generated at the RX input by the RX input impedance ( $Z_{rx}$ ) in the presence of residual SI is explored. SI mitigation circuits in Fig.1 may include a duplex filter and a feed-forward canceler (FFC). An ideal FFC is designed to have a high output impedance, such that the small-signal impedance of  $Z_{rx}$  (often  $50\Omega$ ) will dominate at the RX input. The residual TX-SI modulates any nonlinear resistance and junction capacitance of  $Z_{rx}$ , thus creating  $IM_3$  distortion components.

Distortion introduced by  $Z_{rx}$  should be considered as the residual SI power at RX input is still substantially larger (by 10s of dB) compared with the desired RX signal [4], [8]. Any distortion introduced by  $Z_{rx}$  will add to the nonlinearities produced by the TX-SI passing through the SI mitigation circuits or the intermodulation products produced by the RX chain referenced back to the RX input ( Fig.1). To gain a better understanding of the intermodulation products introduced at the RX input, a model of the nonlinearities associated with  $Z_{rx}$  was created. The residual SI voltage signal at the RX input ( $v_o$ ) can be expressed with a power series expansion of the SI leakage current ( $i_o$ ) shunted into the receiver:

$$v_o = Z_1 i_o + Z_2 i_o^2 + Z_3 i_o^3 + \dots \quad (1)$$

where  $Z_1$  is the small signal impedance of  $Z_{rx}$ , while  $Z_2$  and  $Z_3$  are 2<sup>nd</sup> and 3<sup>rd</sup> order coefficient of  $Z_{rx}$  which describe the 2<sup>nd</sup> and 3<sup>rd</sup> order nonlinearity of  $v_o$ , respectively. For example, if the LNA is a common-gate amplifier,  $Z_1$  is equal to  $1/g_m$  where  $g_m$  is the LNA input device trans-conductance, then  $Z_2$  and  $Z_3$  can also be calculated by using Lagrange's notation

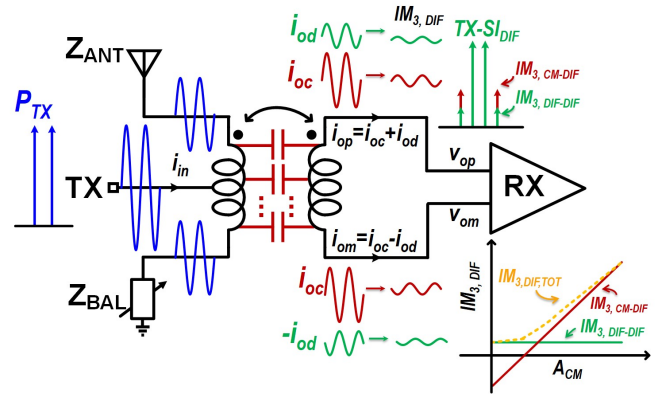


Fig. 2. Capacitive coupling between transformer coils in an EBD. Both differential and common-mode SI leakage current see a nonlinear  $Z_{rx}$ , introducing differential  $IM_3$  at the RX input. Differential  $IM_3$  associated with common-mode dominates with large common-mode TX-SI leakage.

[12], which is related to  $g_{m2}$  and  $g_{m3}$  that are high order coefficients of  $g_m$  [13]. The effect of nonlinear impedance also applies to other LNA topologies, because most LNA's input impedance is a function of  $g_m$ . Thus,  $Z_{rx}$  will introduce non-negligible distortion products at RX input unless the residual TX-SI at the RX input is sufficiently suppressed. The amount of SI suppression and the nonlinear  $Z_{rx}$  should be considered when designing SI mitigation circuits, because the cancellation circuitry output will see the nonlinear  $Z_{rx}$ .

### III. IMPACT OF TX COMMON-MODE LEAKAGE

To further explore the impact of TX leakage on the linearity performance of FD radios, assumptions will be made about the transceiver's air interface. Mainly, the radio assumes use of an integrated EBD. The EBD is based on the matching (electrical balancing) of two impedance — the antenna and a balancing network ( $Z_{BAL}$ ) in a hybrid transformer. This allows splitting the TX output power down the two primary coils which couple to a secondary coil on the receiver side. If the antenna and balancing impedance are well-matched, the SI is suppressed on the RX port. Although an EBD can provide high isolation for differential TX-SI, it has a poor common-mode isolation due to capacitive coupling between the primary and secondary transformer coils (Fig.2). This is problematic from the RX linearity perspective because the common-mode TX leakage will create crossmodulation at  $Z_{rx}$ , producing differential-mode intermodulation products (Fig.2).

A power series expansion of the non-linear  $Z_{rx}$  was used to analyze the effect of common-mode signals at the differential receiver input. The EBD nonlinearity is neglected in the following analytical model. Signals at RX positive ( $v_{op}$ ) and negative ( $v_{om}$ ) input can be written in the following from (1):

$$v_{op} = Z_1(i_{oc} + i_{od}) + Z_2(i_{oc} + i_{od})^2 + Z_3(i_{oc} + i_{od})^3 \quad (2)$$

$$v_{om} = Z_1(i_{oc} - i_{od}) + Z_2(i_{oc} - i_{od})^2 + Z_3(i_{oc} - i_{od})^3 \quad (3)$$

where  $i_{oc}$  and  $i_{od}$  represent common- and differential mode SI leakage current at the RX input, respectively. From (2)

and (3), the differential RX input voltage can be calculated ( $v_o = v_{op} - v_{om}$ ):

$$v_o = Z_1 \cdot 2i_{od} + Z_2 \cdot 4i_{oc}i_{od} + Z_3(2i_{od}^3 + 6i_{oc}^2i_{od}) + \dots \quad (4)$$

We further assume  $i_{oc} = A_{cm}i_{in}$  and  $i_{od} = A_{dif}i_{in}$ ;  $A_{cm}$  and  $A_{dif}$  represent different common- and differential mode TX-to-RX SI current leakage. Then (4) can be written as:

$$v_o = Z_1 \cdot 2A_{dif}i_{in} + Z_2 \cdot 4A_{cm}A_{dif}i_{in}^2 + Z_3(2A_{dif}^3 + 6A_{cm}^2A_{dif})i_{in}^3 + \dots \quad (5)$$

Next, the differential  $IM_3$  generated by applying a current  $i_{in}$  with two tones of equal amplitude ( $S_i$ ) can be expressed as:

$$IM_{3,DIF} = \frac{3}{4}(2A_{dif}^3 + 6A_{cm}^2A_{dif})S_i^3 \quad (6)$$

The second term ( $6A_{cm}^2A_{dif}$ ) associated with the common-mode TX leakage in (6) suggests the common-mode leakage introduces differential nonlinear distortion. The differential component of the residual TX-SI will interact with the common-mode residual TX-SI to produce differential  $IM_3$  distortion. When the common-mode TX-SI leakage is much larger than the differential-mode TX-SI leakage ( $A_{cm} \gg A_{dif}$ ), as would be the case at the EBD output, the differential  $IM_3$  associated with the common-mode leakage dominates at the RX input (shown in Fig.2), which will degrade the RX linearity. Because the TX common-mode leakage generates differential distortion at the RX input, simply designing an LNA and RX chain which is immune to common-mode signals [8], [14] is insufficient to improve the RX linearity. The model describing the differential nonlinear distortion arising from the common-mode TX leakage can be applied to any differential block which experiences a strong common-mode signal. Thus, achieving a high common-mode isolation between the TX and RX is critical in FD transceivers.

#### IV. AIR INTERFACE LINEARITY SIMULATION RESULTS

##### A. Circuit Simulation Model

To verify the TX-SI common-mode to differential distortion conversion model effects on RX linearity performance, a series of circuit-level simulations were performed. The assumed radio front-end (Fig.3) contains an EBD at the air interface to provide differential SI isolation. A tunable balancing impedance  $Z_{BAL}$  realized using a resistive and capacitive bank controlled with integrated switches is necessary to track and match to a dynamic antenna impedance [6]. The RX chain contains an LNA [8], passive mixers, followed by a trans-impedance amplifier (TIA) which then feeds the analog baseband, all modeled using transistor-level schematic simulations. The RF canceler is implemented as an adaptive FIR filter identical to the implementation given in [4], [8].

##### B. Simulation Results

The radio front-end (Fig.3) was implemented in TSMC 40nm process. Simulations were performed using Cadence Spectre combined with Peakview EM simulations to model the passive components. First, simulations were performed

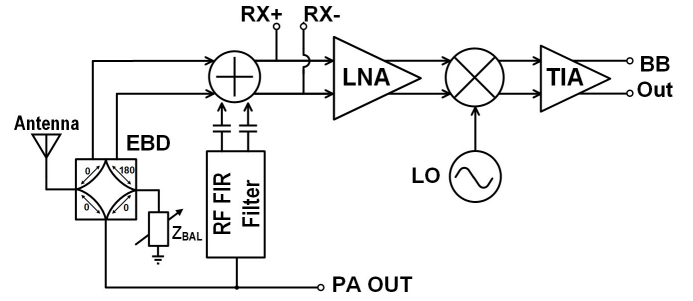


Fig. 3. Block-level diagram of a common full-duplex radio AFE which includes an EBD, a feed-forward canceler, and an LNA followed by a mixer driven by a synthesizer. Simulation results were generated using a transistor-level schematic implementation of this block diagram.

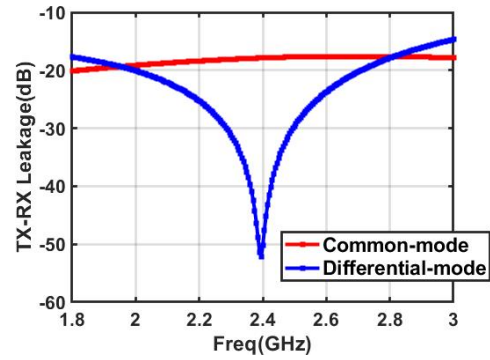


Fig. 4. Simulated differential and common-mode TX-SI attenuation provided by the EBD.

by turning off the canceler which models just the effect of RX input capacitive loading. The EBD  $Z_{BAL}$  was tuned to achieve a maximum TX-RX isolation (Fig.4). The differential SI attenuation provided by the EBD is higher than -40dB over 60MHz bandwidth, while the common-mode SI suppression is only -18dB which is much lower than the differential attenuation. To characterize the EBD and  $Z_{rx}$ 's linearity, two in-band tones were applied to the PA output while the EBD output voltage was measured. Fig.5 shows fundamental and  $IM_3$  components in two different cases: the EBD interfacing to a 50Ω resistor or to the RX chain. When the EBD interfaces to a 50Ω resistor, all the non-linearities are generated by the EBD tuning switches in  $Z_{bal}$ . However, when the EBD is attached to the RX chain and FFC output, the nonlinear  $Z_{rx}$  introduces  $IM_3$  distortion at EBD output, thus degrading the RX linearity performance.

To understand the distortion produced at the differential receiver input from the residual common- and differential-mode TX-SI current applied to a nonlinear  $Z_{rx}$ , an ideal hybrid transformer (Fig.6) is used. Both the residual SI differential and common-mode current signals at the RX input can be controlled by tuning  $R_{BAL}$ ,  $C_1$ , and  $C_2$ . The simulated differential  $IM_3$  at the RX input as a function of differential TX-to-RX SI leakage is shown in Fig.7.  $C_1$  and  $C_2$  are set to zero during the simulation, which has the effect of eliminating a common-

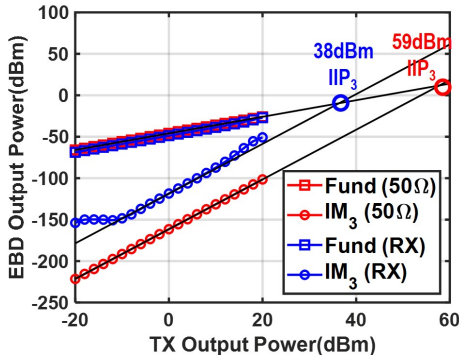


Fig. 5. Linearity testing of the EBD and  $Z_{rx}$  when EBD interfaces to a  $50\Omega$  resistor or the RX chain with two tones at 2.4GHz and 2.42GHz.

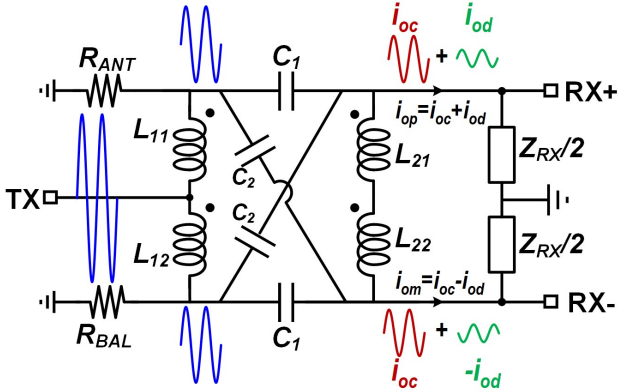


Fig. 6. Hybrid transformer used to model the impact of residual TX-SI on the differential  $IM_3$ . The capacitive-coupling in the transformer produces a common-mode residual TX-SI current which sees a nonlinear  $Z_{rx}$ , generating differential voltage-mode distortion.

mode signal component at the transformer output. The TX output power is set to +15dBm. The  $IP_3$  versus the differential SI leakage referred to TX output is also shown in Fig.7. When the differential SI leakage is increased, the residual differential SI current increases, which introduces more  $IM_3$  distortion and degrades the RX linearity. To meet the linearity requirements of an FD transceiver ( $IP_3$  referred to TX output  $\sim 60$ dBm discussed in Section II), the differential SI must be attenuated by at least 60dB at RF front-end interface.

To understand the effect of common-mode leakage on the RX linearity performance, the differential  $IM_3$  at RX input as a function of common-mode TX-SI is simulated; results are in Fig.8. The differential SI leakage attenuation is set to -60dB. As the common-mode SI leakage increases by 1dB, the differential  $IM_3$  increases by  $\sim 2$ dB which gives good agreement with the relation in (6). The corresponding  $IP_3$  referred to TX output is shown in Fig.8, which further confirms the common-mode SI leakage introduces differential distortion at the RX input, degrading the RX linearity. Thus, a high common-mode isolation ( $>50$ dB) is needed to maintain sufficient RX linearity performance..

Circuit simulation results show that any residual TX-SI,

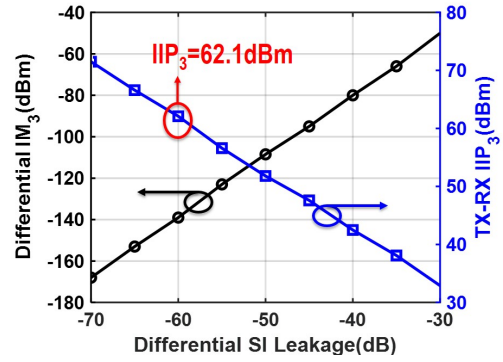


Fig. 7. Simulated differential  $IM_3$  and the corresponding  $IP_3$  referred to TX output versus differential SI leakage when common-mode SI leakage is 0.

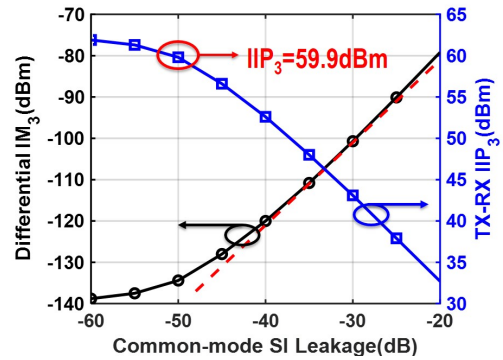


Fig. 8. Simulated differential  $IM_3$  and the corresponding  $IP_3$  referred to TX output versus common-mode SI leakage when differential SI leakage is -60dB.

particularly common-mode SI leakage at RX input, will introduce nonlinear distortion, degrading the RX linearity performance, thus emphasizing the importance to minimize the common-mode TX-SI when designing highly linear SI mitigation circuits (FFC and EBD).

## V. CONCLUSION

This paper explores and models the nonlinear distortion generated at the RX input in full duplex transceivers. An analytical linearity model which describes the degradation of a receiver's linearity at the air interface, due to the RX input impedance, is verified through circuit simulation. Results predict both differential and common-mode SI leakage at RX input introduce differential inter-modulation distortion. The generation of common-to-differential mode nonlinear distortion model can be applied to any differential circuit that has a large common-mode component. This work is the first attempt to model the distortion generated by the RX input impedance which is critical towards understanding the RX performance in the presences of strong self-interference.

## VI. ACKNOWLEDGEMENTS

The authors would like to thank SRC-Intel, CDADIC and Qualcomm for the their contributions as well as Christopher Hull and Farhana Sheikh for their advice.

## REFERENCES

- [1] T. X. Tran, A. Hajisami, P. Pandey, and D. Pompili, "Collaborative mobile edge computing in 5G networks: New paradigms, scenarios, and challenges," *IEEE Commun. Mag.*, vol. 55, no. 4, pp. 54–61, Apr. 2017.
- [2] Y. S. Choi and H. Shirani-Mehr, "Simultaneous transmission and reception: Algorithm, design and system level performance," *IEEE Trans. Wireless Commun.*, vol. 12, no. 12, pp. 5992–6010, 2013.
- [3] D. Bharadia, E. McMillin, and S. Katti, "Full duplex radios," in *Proc. ACM SIGCOMM Conf.*, New York, NY, USA, 2013, pp. 375–386.
- [4] T. Zhang, C. Su, A. Najafi, and J. C. Rudell, "Wideband dual-injection path self-interference cancellation architecture for full-duplex transceivers," *IEEE J. Solid-State Circuits*, vol. 53, no. 6, pp. 1563–1576, 2018.
- [5] B. van Liempd and other, "A +70-dBm IIP3 electrical-balance duplexer for highly integrated tunable front-ends," *IEEE Trans. Microw. Theory Techn.*, vol. 64, no. 12, pp. 4274–4286, Dec. 2016.
- [6] M. Elkholy, M. Mikhemar, H. Darabi, and K. Entesari, "Low-loss integrated passive CMOS electrical balance duplexers with single-ended LNA," *IEEE Trans. Microw. Theory Techn.*, vol. 64, no. 5, pp. 1544–1559, May 2016.
- [7] T. Zhang, A. R. Suvarna, V. Bhagavatula, and J. C. Rudell, "An integrated CMOS passive self-interference mitigation technique for FDD radios," *IEEE J. Solid-State Circuits*, vol. 50, no. 5, pp. 1176–1188, May 2015.
- [8] K. D. Chu, M. Katanbaf, C. Su, T. Zhang, and J. C. Rudell, "A broadband and deep-TX self-interference cancellation technique for full-duplex and frequency-domain-duplex transceiver applications," in *IEEE Int. Solid-State Circuits Conf. (ISSCC) Dig. Tech. Papers*, 2018, pp. 170–172.
- [9] J. Zhou, T. H. Chuang, T. Dinc, and H. Krishnaswamy, "Integrated wideband self-interference cancellation in the RF domain for FDD and full-duplex wireless," *IEEE J. Solid-State Circuits*, vol. 50, no. 12, pp. 3015–3031, 2015.
- [10] D. L. Perez *et al.*, "IEEE 802.11be extremely high throughput: The next generation of wi-fi technology beyond 802.11ax," *IEEE Commun. Mag.*, vol. 57, no. 9, pp. 113–119, Sep. 2019.
- [11] K. D. Chu, M. Katanbaf, C. Su, T. Zhang, and J. C. Rudell, "Integrated CMOS transceivers design towards flexible full duplex (FD) and frequency division duplex (FDD) systems," in *Proc. 2018 IEEE Custom Integrated Circuits Conf. (CICC)*, 2018, pp. 1–11.
- [12] C. C. Morris and R. M. Stark, *Fundamentals of calculus*. Hoboken, NJ: John Wiley Sons, 2015.
- [13] H. Zhang, X. Fan, and E. S. Sinencio, "A low-power, linearized, ultra-wideband LNA design technique," *IEEE J. Solid-State Circuits*, vol. 44, no. 2, pp. 320–330, 2009.
- [14] B. Debaillie and other, "Analog/RF solutions enabling compact full-duplex radios," *IEEE Journal on Selected Areas in Communications (JSAC)*, vol. 32, no. 9, pp. 1662–1673, Jun. 2014.